

Oscillator laser model

Igor E. Protsenko* Alexander V. Uskov

I. E. Protsenko, A. V. Uskov

P.N.Lebedev Physical Institute of the RAS, Moscow 119991, Russia

Email Address: protsenkoie@lebedev.ru, protsenk@gmail.com

Keywords: *nanolasers, inverted oscillators, Heisenberg equations*

A laser model is formulated in terms of quantum harmonic oscillators. Emitters in the low lasing states are usual harmonic oscillators, and emitters in the upper states are *inverted* harmonic oscillators. Diffusion coefficients, consistent with the model and necessary for solving quantum nonlinear laser equations analytically, are found. Photon number fluctuations of the lasing mode and fluctuations of the population of the lasing states are calculated. Collective Rabi splitting peaks are predicted in the intensity fluctuation spectra of the superradiant lasers. Population fluctuation mechanisms in superradiant lasers and lasers without superradiance are discussed and compared with each other.

1 Introduction

Recent technological developments have led to a variety of novel miniature lasers as quantum dot photonic crystal [1, 2, 3, 4, 5, 6, 7], micropillar [8, 9, 10], plasmonic [11] and other kinds of nanolasers [12]. All of them are intensively investigated. The motivation for research of nanolasers is related to fundamental questions, such as general properties of quantum fields with only a few photons in the mode and with practical applications, such as the direct incorporation of lasers into nano-chips [13, 14, 15]. Nanolasers often demonstrate exciting and unusual properties, such as the mode-locking with a repetition rate independent of the cavity length [16, 17].

There is a strong interest in *superradiant* (SR) lasers and nanolasers. Such lasers combine a high gain with a small cavity and operate in the bad-cavity regime [18, 19, 20]. The active medium polarization is a dynamical variable in such lasers, where a collective spontaneous emission into the lasing mode is significant. SR lasers have been experimentally realized with cold alkaline earth atoms [21, 22, 23, 24], rubidium atoms [25], and quantum dots [26] as the active medium. SR lasers are less sensitive to the cavity-length fluctuations important for atomic clocks [21, 22, 25]. Superradiance leads to interesting collective effects, such as excitation trapping [23, 25] and superthermal photon statistics [10, 26, 27], with possible applications in high-visibility optical imaging [28].

Analytical description of SR lasers meets difficulties. Quantum noise in such lasers is not a perturbation, the laser equations are nonlinear, and the active medium polarization is a dynamical variable not eliminated adiabatically. Strong population fluctuations in SR lasers play a significant role in laser dynamics leading to large relaxation oscillations [29] and the acceleration of spontaneous emission into the lasing mode [30]. High population fluctuations at superradiance were noted previously, for example, at a generation of superradiant pulses [31].

The first purpose of the present work is to continue calculations and investigation of the population fluctuations in SR lasers at a low excitation using the approach of [29, 30, 32, 33]. The laser at a low excitation does not generate coherent radiation and operates as a LED or, if the collective spontaneous emission (the superradiance) into the lasing mode is significant, as SR LED.

Calculations and investigation of the population fluctuations are necessary for better understanding properties of SR LEDs and lasers, for solving nonlinear laser equations [30], and for finding quantum characteristics of nanolasers as, for example, the autocorrelation function g_2 of the lasing field, widely used in experiments and the theory [34].

Our previous papers [32, 33], neglected population fluctuations at low laser excitation. In [29], population fluctuations have been taken into account at a high excitation when the laser generates coherent radiation then laser equations can be solved by the usual perturbation procedure. The procedure of [29] cannot account for population fluctuations at a low laser excitation. The paper [30] describes the treatment of nonlinearities and population fluctuations at a low laser excitation. However, the analysis in [30]

arXiv:2206.05452v2 [quant-ph] 22 Nov 2022

was simplified and restricted by a very low laser excitation when population fluctuations determined by only the pump and the decay of the upper lasing states but practically do not depend on the lasing field. The restriction of analysis in [30] appears because of the difficulty in finding diffusion coefficients consistent with the approximate equations. It turns out that the use of well-known diffusion coefficients found from generalized Einstein relations (GER) leads to inconsistencies in the results of the approximate equations, for example, the breaking of Bose-commutation relations for the lasing field operator [29]. The fact that different approximate approaches in quantum optics require different diffusion coefficients is well-known. For example, some diffusion coefficients change in the transition from operator to c-number Langevin equations – see the discussion in section 12.3 in [35].

Another purpose of this paper, necessary for continuing research [30], is to find diffusion coefficients consistent with our approximate equations. It will be done with the help of an *oscillator laser model* (OLM), representing the laser as a combination of the usual and *inverted* harmonic oscillators. The model of optical media as a set of oscillators is used widely in nonlinear optics [36, 37]. Glauber introduced inverted oscillators for the modelling pump bath [38]. Inverted oscillators found applications in the quantum theory of linear amplifiers [39]. There is a difference between the quantum theory of linear amplifiers [39] and OLM. OLM does not eliminate the active medium polarisation adiabatically, quantum theory of linear amplifiers does this.

OLM leads to the same quantum laser equations as in [29, 30, 33], finds correct diffusion coefficients in the frame of the input-output theory [40, 41] and preserves Bose commutation relations for the field operators. The results of OLM let us find population fluctuations in the first-order approximation.

Using approximate analytical equations with appropriate diffusion coefficients, we find and investigate the photon number and the population fluctuations, their spectra, and variances; describe sources of population fluctuations and compare population fluctuations in the SR LEDs and the LEDs without SR.

Section 2 is introductory. There we describe the exact and approximate two-level laser models. In subsection 2.1, we describe the approximate approach and derive Eqs. (30) – (32) for fluctuations of binary operators.

Section 3 describes the oscillator laser model.

Section 4 presents the calculation of diffusion coefficients for Eqs. (30) – (32) consistent with the approximation when population fluctuations are neglected. There we find the population fluctuation spectrum in the first-order approximation.

Section 5 contains results about the population fluctuation spectra and variances; describes the influence of population fluctuations on the field intensity fluctuation spectra. This section discusses the mechanisms of population fluctuations and the comparison of population fluctuations in SR LEDs and LEDs without SR.

Concluding section 6 summarises the results.

For convenience, Table 1 shows definitions of operators, variables, and parameters with references to equations where the operator or the parameter appears in the main text. Table 1 does not include fluctuation operators, denoted by the symbol δ , and mean values marked by the same letter as the operator.

For example, there are no mean values like $\Sigma = \langle \hat{\Sigma} \rangle$ and fluctuation operators like $\delta \hat{\Sigma} = \hat{\Sigma} - \Sigma$.

2 Quantum lwo-level laser model

We consider a lasing medium with a large number $N_0 \gg 1$ of the two-level identical emitters in the optical cavity with the cavity mode resonant to the emitter transitions, shown schematically in Fig. 1. Emitters are fixed in space as in quantum dot lasers [26, 42]. We investigate the stationary case when, on average, N_g emitters are in their ground states and N_e emitters are in their excited states. The incoherent pump maintains the number of emitters in the excited states and the stationary population inversion $N = N_e - N_g$, compensating for the energy losses.

We consider a *weak excitation* of the lasing medium when: (a) the number of photons in the cavity is less or of the order of one and (b) there is no population inversion in the lasing medium. There is no

Table 1: Definitions of operators and parameters

Symbol	Definition	Eq.	Symbol	Definition	Eq.
\hat{a}	lasing mode amplitude of i-th emitter	(1)	$\hat{\sigma}_i^+$ ($\hat{\sigma}_i$)	rising (lowering) operator of i-th emitter	(1)
\hat{n}_i^e (\hat{n}_i^g)	operator of population of excited (ground) state of i-th emitter	(2)	\hat{v}	active medium polarisation operator	(3), (43)
\hat{N}_e (\hat{N}_g)	operator of population of all excited (ground) states	(3)	N	mean population inversion	Sec. 1
\hat{F}_α	Langevin force operator $\alpha = \{a, v, N_e, N_g, \dots\}$	(4), (5), etc.	$\hat{\Sigma}$	field-polarization interaction energy operator	(7), (50)
\hat{n}	photon number operator	(25)	\hat{D}	dipole-dipole interaction energy operator	(28)
\hat{b}_i (\hat{c}_i)	Bose-operator for i-th emitter in the excited (ground) state	(36)	\hat{b} (\hat{c})	Bose-operator for N_e (N_g) emitters in the excited (ground) states	(37)
\hat{a}_{in}	laser field bath Bose-operator	(39)	\hat{b}_{in} , \hat{c}_{in}	polarisation baths Bose-operators	(40), (41)
\hat{D}_f	dipole-dipole interaction energy in terms of Bose-operators	(55)	$\hat{\Gamma}$	interaction with bath environments	(1), (36)
$\hat{\alpha}(\omega)$	Fourier-component operator for $\hat{\alpha}(t)$, $\alpha = \{a, v, \dots\}$	(19)	$\delta\hat{\alpha}(\omega)$	Fourier-component operator for fluctuations $\delta\hat{\alpha}(t)$, $\alpha = \{n, \Sigma, D, \dots\}$	(59)
Ω	vacuum Rabi frequency	(1)	f_i	normalized coupling strength of i-th emitter with lasing mode	(1)
f_{bi} (f_{ci})	normalized coupling strength of i-th emitter in excited (ground) state	(36)	f_b (f_c)	average normalised coupling strength of emitter in excited (ground) state	(37)
f	average emitter-field coupling strength	(8), (48)	γ_\perp	polarisation decay rate	(5)
N_0	total number of emitters	(1)	κ	lasing mode amplitude decay rate	(4)
γ_\parallel	upper level population decay rate	(6)	P	upper level dimensionless pump rate, normalized to γ_\parallel	(6)
$2D_{\alpha\beta}$	diffusion coefficient for Langevin force	(17)	γ_P	population fluctuation decay rate	(12)
N_{th}	threshold population inversion in semiclassical laser theory	(21)	$n(\omega)$	laser field spectrum	(20)
ω_0	optical carrier frequency	(1), (36)	ω	deviation from ω_0 in $n(\omega)$; frequency of intensity, etc. fluctuations	(19), (59)
ω_{opt}	optical field frequency	after (21)			
$(\hat{a}\delta\hat{N}_e)_\omega$	Fourier-component of $\hat{a}\delta\hat{N}_e$	(22)	$S_{aN_e}(\omega)$	power spectrum of $\hat{a}\delta\hat{N}_e$	(22), (23)
$\delta^2n(\omega)$	photon number fluctuation spectrum	(60), (67)	δ^2n	photon number fluctuation dispersion	(63)
$\delta^2N_e(\omega)$	population fluctuation spectrum	(61)	δ^2N_e	population fluctuation dispersion	(64)
$S_\Sigma(\omega)$	auxiliary function	(61), (68)	$S(\omega)$	auxiliary function	(61), (69)

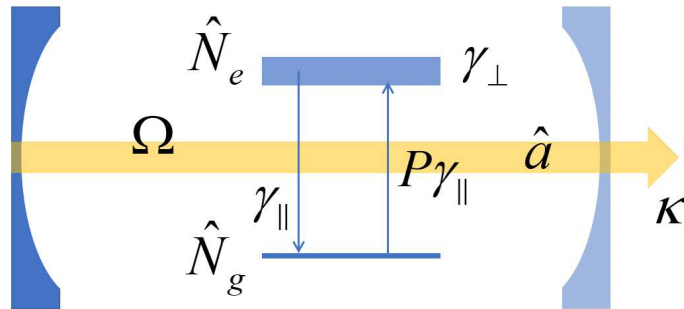


Figure 1: Scheme of the two-level laser. The population of the upper levels of emitters decays to the low levels with the rate γ_\parallel and is pumped with the rate $\gamma_\parallel P$ from the low levels. The lasing mode decays through the semi-transparent mirror with the rate κ and resonantly interacts with lasing transitions of two-level emitters with the vacuum Rabi frequency Ω .

generation of coherent radiation in such a regime, so the laser operates as a LED. We will call it a weak pump – the pump providing the weak excitation regime.

We write Hamiltonian of the two-level laser, similar to the one used (maybe in different notations) in many papers and books, as [29, 30, 32, 33, 35, 43, 44], written in the interaction picture with the carrier frequency ω_0 and the RWA approximation

$$H = i\hbar\Omega \sum_{i=1}^{N_0} f_i \left(\hat{a}^+ \hat{\sigma}_i - \hat{\sigma}_i^+ \hat{a} \right) + \hat{\Gamma}. \quad (1)$$

Here Ω is the vacuum Rabi frequency; f_i describes the difference in couplings of different emitters with the lasing mode, \hat{a} is the Bose operator of the lasing mode amplitude, $\hat{\sigma}_i$ is the lowering operator of i -th emitter [43], $\hat{\Gamma}$ describes the interaction of the lasing mode and emitters with the white noise baths of the environment.

Non-zero commutation relations for operators are [29, 30, 32, 33, 43]

$$[\hat{a}, \hat{a}^+] = 1, \quad [\hat{\sigma}_i, \hat{\sigma}_j^+] = (\hat{n}_i^g - \hat{n}_i^e) \delta_{ij}, \quad [\hat{\sigma}_i, \hat{n}_j^e] = [\hat{n}_j^g, \hat{\sigma}_i] = \delta_{ij} \hat{\sigma}_i, \quad (2)$$

where \hat{n}_j^e and \hat{n}_j^g are operators of populations of the upper and the low levels of the i -th emitter, δ_{ij} is the Kronecker symbol.

Following [29, 30, 33], we introduce operators \hat{v} and $\hat{N}_{e,g}$ of the polarization and populations of all emitters

$$\hat{v} = \sum_{i=1}^{N_0} f_i \hat{\sigma}_i, \quad \hat{N}_{e,g} = \sum_{i=1}^{N_0} \hat{n}_i^{e,g}. \quad (3)$$

Using commutation relations (2) and Hamiltonian (1), we write Maxwell-Bloch equations for \hat{a} , \hat{v} , and \hat{N}_e

$$\dot{\hat{a}} = -\kappa \hat{a} + \Omega \hat{v} + \hat{F}_a \quad (4)$$

$$\dot{\hat{v}} = -(\gamma_{\perp}/2) \hat{v} + \Omega f \hat{a} (2\hat{N}_e - N_0) + \hat{F}_v \quad (5)$$

$$\dot{\hat{N}}_e = -\Omega \hat{\Sigma} + \gamma_{\parallel} [P (N_0 - \hat{N}_e) - \hat{N}_e] + \hat{F}_{N_e}, \quad (6)$$

where

$$\hat{\Sigma} = \hat{a}^+ \hat{v} + \hat{v}^+ \hat{a}, \quad (7)$$

κ , γ_{\perp} and γ_{\parallel} are decay rates, $P\gamma_{\parallel}$ is the pump rate. We call dimensionless P a normalized pump; \hat{F}_{α} with the index $\alpha = \{a, v, N_e\}$ are Langevin forces of the white noise baths. The total number of emitters is preserved, so $\hat{N}_e + \hat{N}_g = N_0$. In Eqs. (4) – (6) we approximate

$$f_i^2 \approx f = N_0^{-1} \sum_{i=1}^{N_0} f_i^2. \quad (8)$$

Physically, $\hat{\Sigma}$ is the operator of a normalized field-polarisation interaction energy analogous to the field-assisted polarisation [26, 45]. An operator similar to $\hat{\Sigma}$ has been used previously, for example, in [46]. We rewrite Eqs. (4) – (6) in the form convenient for our calculations. We separate the operator mean values and fluctuations

$$\hat{N}_{e,g} = N_{e,g} + \delta \hat{N}_{e,g}, \quad \hat{\Sigma} = \Sigma + \delta \hat{\Sigma} \quad (9)$$

and write instead of Eqs. (4) – (6)

$$\dot{\hat{a}} = -\kappa \hat{a} + \Omega \hat{v} + \hat{F}_a \quad (10)$$

$$\dot{\hat{v}} = -(\gamma_{\perp}/2) \hat{v} + \Omega f (\hat{a} N + 2\hat{a} \delta \hat{N}_e) + \hat{F}_v. \quad (11)$$

$$\delta \dot{\hat{N}}_e = -\Omega \delta \hat{\Sigma} - \gamma_P \delta \hat{N}_e + \hat{F}_{N_e}, \quad (12)$$

where $\gamma_P = \gamma_{\parallel}(P + 1)$ and

$$0 = -\Omega\Sigma + \gamma_{\parallel} [P(N_0 - N_e) - N_e]. \quad (13)$$

Diffusion coefficients for correlations of Langevin forces in Eq. (10) – (12) are well-known [43, 47] and derived from generalized Einstein relations [48].

We take the stationary mean photon number $n = \langle \hat{a}^+ \hat{a} \rangle$ and find from Eq. (10) $0 = -2\kappa n + \Omega\Sigma$. The last equation and Eq. (13) lead to the energy conservation law

$$2\kappa n = \gamma_{\parallel} [P(N_0 - N_e) - N_e]. \quad (14)$$

Nonlinear quantum equations (10) – (12), supplemented by Eqs. (7), (13), and (14) are our basic set of equations [29, 30, 33]. This set is exact (in the frame of the two-level laser model), but it is hard to solve it analytically. We consider the stationary case and solve this set of equations by the approximate analytical approach described in the next subsection.

2.1 Approximate analytical approach

One can find an approximate analytical solution of Eqs. (10) – (12) neglecting population fluctuations. We call this approach a zero-order approximation respectively to population fluctuations or simply a zero-order approximation. Taking $\delta\hat{N}_e = 0$, we reduce the set (10) – (12) to two linear, on \hat{a} and \hat{v} , equations

$$\dot{\hat{a}} = -\kappa\hat{a} + \Omega\hat{v} + \hat{F}_a \quad (15)$$

$$\dot{\hat{v}} = -(\gamma_{\perp}/2)\hat{v} + \Omega f N \hat{a} + \hat{F}_v. \quad (16)$$

Non-zero diffusion coefficients $2D_{\alpha\beta}$ for Langevin forces in

$$\langle \hat{F}_{\alpha}(t) \hat{F}_{\beta}(t') \rangle = 2D_{\alpha\beta} \delta(t - t') \quad (17)$$

in Eqs. (15), (16) are [29]:

$$2D_{aa^+} = 2\kappa, \quad 2D_{vv^+} = \gamma_{\perp} f N_g, \quad 2D_{v^+v} = \gamma_{\perp} f N_e. \quad (18)$$

Diffusion coefficients $2D_{vv^+}$ and $2D_{v^+v}$ are different from the "exact" ones found from GER when $\hat{N}_{e,g}$ are operators. We call diffusion coefficients (18), and the others found for the zero-order approximation equations as zero-order diffusion coefficients. With diffusion coefficients (18), Bose commutation relations for \hat{a} found from Eqs. (15), (16) are preserved.

One can solve linear Eqs. (15), (16) by the Fourier-transform

$$\hat{a}(t) = \frac{1}{\sqrt{2\pi}} \int_{-\infty}^{\infty} \hat{\alpha}(\omega) e^{-i\omega t} d\omega, \quad (19)$$

where $\alpha = \{a, v\}$ and calculate the field spectrum $n(\omega)$

$$\langle \hat{a}^+(\omega) \hat{a}(\omega') \rangle = n(\omega) \delta(\omega + \omega'). \quad (20)$$

It was found in [29] that

$$n(\omega) = \frac{(\kappa\gamma_{\perp}^2/2)N_e/N_{th}}{[(1 - N/N_{th})(\kappa\gamma_{\perp}/2) - \omega^2]^2 + \omega^2(\kappa + \gamma_{\perp}/2)^2}, \quad (21)$$

where $N_{th} = 2\Omega^2 f / \kappa\gamma_{\perp}$ is the threshold population inversion found in the semiclassical laser theory. The lasing field operator is $\hat{a}e^{-i\omega_0 t}$, so the frequency ω in Eqs. (19) – (21) is the *deviation* from the optical carrier frequency ω_0 . The field spectrum (21), expressed in terms of the optical frequency $\omega_{opt} = \omega_0 + \omega$, is $n(\omega_{opt} - \omega_0)$. Fig. 3 shows examples of the field spectra $n(\omega_{opt} - \omega_0)$.

With the help of Eq. (21), we find the mean photon number $n = (2\pi)^{-1} \int_{-\infty}^{\infty} n(\omega) d\omega$ as a function of N_e . Then N_e can be determined from the energy conservation law (14) as in [29, 30, 32, 33].

Zero-order approximation leads to interesting results, as the mean photon number $n(P)$ for SR laser, found beyond the quantum rate equation approach of [49, 50], i.e. without adiabatic elimination of polarization; collective Rabi splitting in the laser field spectra [29, 30, 33]. Solving Eqs. (15), (16) by Fourier transform, one can easily see that the second-order autocorrelation function $g_2 \equiv \langle \hat{a}^+ \hat{a}^+ \hat{a} \hat{a} \rangle / n^2 = 2$ in this zero-order approximation. One can suppose, therefore, that the super-thermal photon statistics with $g_2 > 2$ in the SR LEDs [10, 26, 27] is due to population fluctuations neglected in Eqs. (15), (16).

Recognizing the importance of population fluctuations in SR LEDs and lasers, we come in [30] to a first-order approximation, which includes population fluctuations.

In the first-order approximation, we take into account the nonlinear term $\hat{a} \delta \hat{N}_e$ in Eq. (11) and calculate $\delta \hat{N}_e$. We consider the product $\hat{a} \delta \hat{N}_e$ as a random variable with the Fourier-component operator $(\hat{a} \delta \hat{N}_e)_\omega$ and the power spectrum $S_{aN_e}(\omega)$,

$$\langle (\hat{a}^+ \delta \hat{N}_e)_\omega (\hat{a} \delta \hat{N}_e)_{\omega'} \rangle = S_{aN_e}(\omega) \delta(\omega + \omega'). \quad (22)$$

It was shown in [30] that $S_{aN_e}(\omega)$ is a convolution of the field spectrum $n(\omega)$ and the population fluctuation spectrum $\delta^2 N_e(\omega)$

$$S_{aN_e}(\omega) = \frac{1}{2\pi} \int_{-\infty}^{\infty} n(\omega - \omega') \delta^2 N_e(\omega') d\omega'. \quad (23)$$

A way for analytical calculation of $S_{aN_e}(\omega)$ is that $n(\omega)$ and $\delta^2 N_e(\omega)$ in Eq. (23) are found in the zero-order approximation. So we calculate approximate $S_{aN_e}(\omega)$ from Eq. (23) and then find the first-order approximation solution of Eqs. (10) – (12) in terms of Fourier-component operators [30].

In [30], we presented a simplified version of the first-order approximation, supposing so weak excitation that the first term on the right in Eq. (12) can be neglected, and Eq. (12) is approximately replaced by

$$\delta \dot{\hat{N}}_e \approx -\gamma_P \delta \hat{N}_e + \hat{F}_{N_e}. \quad (24)$$

This equation can be easily solved.

In [30], we found that population fluctuations in SR LEDs significantly enhance spontaneous emission into the lasing mode at certain conditions, increasing the LED radiation. This result confirms the importance of population fluctuations in SR LEDs and lasers. It encourages us to continue working with the first-order approximation, mainly to carry it out without Eq. (12) replacement by Eq. (24).

To find population fluctuations, in this case, we must know $\delta \hat{\Sigma}$. For this, we take Eqs. (15), (16) and, applying the rule of the differentiation of products, write equations

$$\dot{\hat{n}} = -2\kappa \hat{n} + \Omega \hat{\Sigma} + \hat{F}_n \quad (25)$$

$$\dot{\hat{\Sigma}} = -(\kappa + \gamma_\perp/2) \hat{\Sigma} + 2\Omega f (\hat{n} N + \hat{D} + N_e) + \hat{F}_\Sigma \quad (26)$$

$$\dot{\hat{D}} = -\gamma_\perp \hat{D} + \Omega N \hat{\Sigma} + \hat{F}_D, \quad (27)$$

for the photon number operator $\hat{n} = \hat{a}^+ \hat{a}$, $\hat{\Sigma}$, given by Eq. (7), and

$$\hat{D} = f^{-1} \sum_{i \neq j} f_i f_j \hat{\sigma}_i^+ \hat{\sigma}_j, \quad (28)$$

which is normalized dipole-dipole interaction energy of different emitters [29, 30, 33]. \hat{F}_α , $\alpha = \{n, \Sigma, D\}$ are Langevin forces.

We separate fluctuations and the mean values in operators

$$\hat{n} = n + \delta \hat{n}, \quad \hat{\Sigma} = \Sigma + \delta \hat{\Sigma}, \quad \hat{D} = D + \delta \hat{D}, \quad (29)$$

insert Eqs. (29) into Eqs. (25) – (27), obtain equations for fluctuations

$$\delta \dot{\hat{n}} = -2\kappa \delta \hat{n} + \Omega \delta \hat{\Sigma} + \hat{F}_n \quad (30)$$

$$\delta \dot{\hat{\Sigma}} = -(\kappa + \gamma_\perp/2) \delta \hat{\Sigma} + 2\Omega f (\delta \hat{n} N + \delta \hat{D}) + \hat{F}_\Sigma \quad (31)$$

$$\delta \dot{\hat{D}} = -\gamma_\perp \delta \hat{D} + \Omega N \delta \hat{\Sigma} + \hat{F}_D \quad (32)$$

and the set of algebraic equations for the mean values n , Σ and D

$$0 = -2\kappa n + \Omega\Sigma \quad (33)$$

$$0 = -(\kappa + \gamma_{\perp}/2)\Sigma + 2\Omega f(nN + D + N_e) \quad (34)$$

$$0 = -\gamma_{\perp}D + \Omega N\Sigma. \quad (35)$$

n , Σ , D and $N_{e,g}$ found from Eqs. (33) – (35) (with the energy conservation law (14) and the relation $N_e + N_g = N_0$) are the same as the ones found from Eqs. (10), (11) [29, 33].

In the next steps of the procedure, we must solve linear Eqs. (30) – (32) by the Fourier-transform, find $\delta\hat{\Sigma}$, find $\delta\hat{N}_e(\omega)$ from Eq. (12) and calculate $\delta^2 N_e(\omega)$ in Eq. (23). For doing this, we must know diffusion coefficients for Langevin forces in Eqs. (30) – (32).

An essential part of our procedure is calculating the zero-order diffusion coefficients for Langevin forces in Eqs. (30) – (32). In these equations (as well as in Eqs. (15), (16)), we can not use "exact" diffusion coefficients found from GER; they will be inconsistent, as we will see, with the results of Eqs. (15), (16). Calculation of the zero-order diffusion coefficients for Langevin forces in Eqs. (30) – (32) is carried out below in the frame of the oscillator laser model described in the next section.

3 Laser equations in terms of oscillators

Two zero-order diffusion coefficients $2D_{vv^+}$ and $2D_{v^+v}$ for Langevin forces in Eqs. (15), (16) have been determined in [30, 33] from GER by setting populations to be constants (i.e. not operators). We found it difficult to determine *five* zero-order diffusion coefficients for Langevin forces in Eqs. (25) – (27) or (30) – (32) similar way. It turns out to be easier to use a zero-order approximation *Hamiltonian* H_0 leading to Eqs. (25) – (27) or (30) – (32). The properties of operators in H_0 help us to find diffusion coefficients for any equations of the zero-order approximation.

Hamiltonian H_0 can be obtained in an *oscillator laser model* (OLM). This model describes N_g emitters in the ground states as conventional (normal) quantum harmonic oscillators with Bose operators $\hat{c}_i e^{-i\omega_0 t}$, $i = 1 \dots N_g$. We will describe N_e emitters in the upper states as *inverted* harmonic oscillators with Bose operators $\hat{b}_j e^{+i\omega_0 t}$, $j = 1 \dots N_e$. Note the sign "+" in the exponent multiplier $e^{+i\omega_0 t}$ for the inverted oscillator, while the sign "-" in the multiplier $e^{-i\omega_0 t}$ is for the usual, non-inverted oscillator. \hat{b}_j and \hat{c}_j are changed in time much slower than $e^{-i\omega_0 t}$. The normal and the inverted oscillators are shown schematically in Fig. 2.

Hamiltonian H_0 of the OLM, written in the interaction picture and the RWA with the carrier frequency ω_0 is

$$H_0 = i\hbar\Omega \left[\hat{a}^+ \left(\sum_{i=1}^{N_e} f_{bi} \hat{b}_i^+ + \sum_{i=1}^{N_g} f_{ci} \hat{c}_i \right) - h.c. \right] + \hat{\Gamma}. \quad (36)$$

Here dimensionless factors $f_{b,ci}$ describe the difference in couplings of different oscillators with the field; the rest of the notations is the same as for the "exact" two-level laser Hamiltonian (1).

We represent H_0 in terms of only three oscillators with Bose operators \hat{a} , \hat{b} and \hat{c}

$$\hat{b} = f_b^{-1} \sum_{i=1}^{N_e} f_{bi} \hat{b}_i, \quad \hat{c} = f_c^{-1} \sum_{i=1}^{N_g} f_{ci} \hat{c}_i, \quad f_{b,c} = \left(\sum_{i=1}^{N_{e,g}} f_{b,ci}^2 \right)^{1/2}. \quad (37)$$

Bose commutation relations $[\hat{b}, \hat{b}^+] = [\hat{c}, \hat{c}^+] = 1$ follow from Bose commutation relations for \hat{b}_i and \hat{c}_i . Hamiltonian (36), in terms of three oscillators, reads

$$H_0 = i\hbar\Omega \left[f_b(\hat{a}^+ \hat{b}^+ - \hat{a} \hat{b}) + f_c(\hat{a}^+ \hat{c} - \hat{c}^+ \hat{a}) \right] + \hat{\Gamma}. \quad (38)$$

Hamiltonian (38) and Bose-commutation relations lead to Heisenberg-Langevin equations for \hat{a} , \hat{b}^+ and \hat{c}

$$\dot{\hat{a}} = -\kappa \hat{a} + \Omega \left(f_b \hat{b}^+ + f_c \hat{c} \right) + \sqrt{2\kappa} \hat{a}_{in} \quad (39)$$

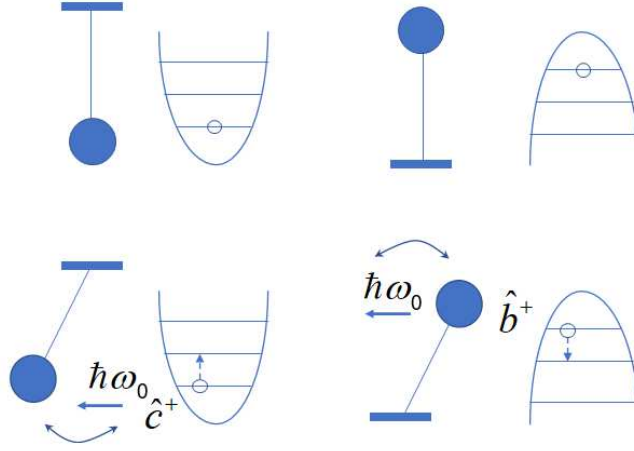


Figure 2: When the conventional oscillator (on the left) accepts the energy quantum $\hbar\omega_0$, it comes from the ground state to the first excited state. The inverted oscillator (on the right) loses a quantum and comes from its "inverted ground" state with the maximum energy to the first de-excited state. In the OLM, we consider virtual transitions, shown by arrows at the bottom of the figure and described by operators \hat{b}^+ for the inverted and \hat{c}^+ for the conventional oscillator, see Hamiltonian (38). We neglect changes in populations of levels and consider dynamics of the polarization of oscillators, see the discussion at the end of section 5.

$$\dot{\hat{b}}^+ = -(\gamma_{\perp}/2)\hat{b}^+ + \Omega f_b \hat{a} + \sqrt{\gamma_{\perp}} \hat{b}_{in}^+ \quad (40)$$

$$\dot{\hat{c}} = -(\gamma_{\perp}/2)\hat{c} - \Omega f_c \hat{a} + \sqrt{\gamma_{\perp}} \hat{c}_{in}, \quad (41)$$

where \hat{a}_{in} , \hat{b}_{in} and \hat{c}_{in} are Bose-operators of baths. Non-zero correlations between the bath operators are

$$\langle \hat{\alpha}_{in}(t) \hat{\alpha}_{in}^+(t') \rangle = \delta(t - t'), \quad (42)$$

where $\hat{\alpha}_{in} = \{\hat{a}_{in}, \hat{b}_{in}, \hat{c}_{in}\}$. Operators of different baths do not correlate with each other. Langevin forces with the bath operators are added in Eqs. (39) – (41) following the input-output theory [40, 41].

We simplify Eqs. (39) – (41) by introducing an operator

$$\hat{v} = f_b \hat{b}^+ + f_c \hat{c} \quad (43)$$

of the polarization of the lasing medium (using the same notation \hat{v} as in Eq. (3)), and re-write Eqs. (39) – (41)

$$\dot{\hat{a}} = -\kappa \hat{a} + \Omega \hat{v} + \sqrt{2\kappa} \hat{a}_{in} \quad (44)$$

$$\dot{\hat{v}} = -(\gamma_{\perp}/2) \hat{v} + \Omega (f_b^2 - f_c^2) \hat{a} + \hat{F}_v, \quad (45)$$

with the Langevin force

$$\hat{F}_v = \sqrt{\gamma_{\perp}} (f_b \hat{b}_{in}^+ + f_c \hat{c}_{in}). \quad (46)$$

Langevin forces are delta-correlated $\langle \hat{F}_{\alpha}(t) \hat{F}_{\beta}(t') \rangle = 2D_{\alpha\beta} \delta(t - t')$ with diffusion coefficients

$$2D_{v+v} = \gamma_{\perp} f_b^2, \quad 2D_{vv^+} = \gamma_{\perp} f_c^2, \quad 2D_{v+v} = 2D_{vv^+} = 0, \quad (47)$$

followed from Eqs. (42), (43) and (46). We approximate

$$f_{b,c}^2 \approx f N_{e,g}, \quad f = N_0^{-1} \left(\sum_{i=1}^{N_e} f_{bi}^2 + \sum_{i=1}^{N_g} f_{ci}^2 \right), \quad (48)$$

where N_e , (N_g) are the mean numbers of emitters in the ground (in the excited) states, and $N_0 = N_e + N_g$ is the total number of emitters. With the approximation (48), equations (44), (45) became identical with equations (15), (16) and diffusion coefficients (47) – with diffusion coefficients (18). Such a coincidence confirms the correctness of the OLM.

4 Diffusion coefficients and population fluctuations

Now we will see that the OLM leads to Eqs. (30) – (32) and obtain diffusion coefficients for these equations. For this, using Eqs. (44), (45) and the rule of differentiation of products, we write the equation of motion for $\hat{n} = \hat{a}^+ \hat{a}$

$$\dot{\hat{n}} = -2\kappa\hat{n} + \Omega\hat{\Sigma} + \hat{F}_n, \quad (49)$$

where

$$\hat{\Sigma} = f_b (\hat{b}\hat{a} + \hat{a}^+\hat{b}^+) + f_c (\hat{c}^+\hat{a} + \hat{a}^+\hat{c}), \quad (50)$$

and the Langevin force

$$\hat{F}_n = \sqrt{2\kappa} (\hat{a}_{in}^+ \hat{a} + \hat{a}^+ \hat{a}_{in}). \quad (51)$$

In Eqs. (7), (50), and below, we use the same notation Σ for the normalized field-polarization interaction energy. We write, using Eqs. (44), (45),

$$\dot{\hat{\Sigma}} = -(\kappa + \gamma_{\perp}/2)\hat{\Sigma} + 2\Omega [\hat{n} (f_b^2 - f_c^2) + \hat{D}_f + f_b^2] + \hat{F}_{\Sigma}, \quad (52)$$

where

$$\hat{D}_f = f_b^2 \hat{b}^+ \hat{b} + f_c^2 \hat{c}^+ \hat{c} + f_b f_c (\hat{c}^+ \hat{b}^+ + \hat{c} \hat{b}), \quad (53)$$

and the Langevin force

$$\begin{aligned} \hat{F}_{\Sigma} = & \sqrt{2\kappa} f_b (\hat{b} \hat{a}_{in} + \hat{b}^+ \hat{a}_{in}^+) + \sqrt{\gamma_{\perp}} f_b (\hat{b}_{in} \hat{a} + \hat{b}_{in}^+ \hat{a}^+) + \\ & \sqrt{2\kappa} f_c (\hat{c}^+ \hat{a}_{in} + \hat{a}_{in}^+ \hat{c}) + \sqrt{\gamma_{\perp}} f_c (\hat{c}_{in}^+ \hat{a} + \hat{a}^+ \hat{c}_{in}). \end{aligned} \quad (54)$$

With the derivation of Eq. (52), we set the normal ordering of Bose operators replacing $f_b^2 \hat{a} \hat{a}^+$ with $f_b^2 \hat{a}^+ \hat{a} + f_b^2$. We obtain the equation for \hat{D}_f

$$\dot{\hat{D}}_f = -\gamma_{\perp} \hat{D}_f + \Omega (f_b^2 - f_c^2) \hat{\Sigma} + \hat{F}_{D_f} \quad (55)$$

with the Langevin force

$$\begin{aligned} \hat{F}_{D_f} = & \sqrt{\gamma_{\perp}} [f_b^2 (\hat{b}_{in}^+ \hat{b} + \hat{b}^+ \hat{b}_{in}) + f_c^2 (\hat{c}_{in}^+ \hat{c} + \hat{c}^+ \hat{c}_{in}) + \\ & f_b f_c (\hat{c}_{in}^+ \hat{b}^+ + \hat{c}^+ \hat{b}_{in}^+ + \hat{c}_{in} \hat{b} + \hat{c} \hat{b}_{in})] \end{aligned} \quad (56)$$

in the same way as equations for \hat{n} and $\hat{\Sigma}$.

Eqs. (49), (52) and (55) are the set of linear equations for \hat{n} , $\hat{\Sigma}$ and \hat{D}_f . Delta-correlations for Langevin forces in these equations have non-zero diffusion coefficients

$$\begin{aligned} 2D_{nn} = 2\kappa n, \quad 2D_{\Sigma\Sigma} = 2\kappa D_f + \gamma_{\perp} (f_b^2 + f_c^2) n + (2\kappa + \gamma_{\perp}) f_b^2 \\ 2D_{D_f D_f} = \gamma_{\perp} [(f_c^2 + f_b^2) D_f + 2f_b^2 f_c^2], \\ 2D_{\Sigma n} = 2D_{n\Sigma} = \kappa \Sigma, \quad 2D_{\Sigma D_f} = 2D_{D_f \Sigma} = (\gamma_{\perp}/2)(f_b^2 + f_c^2) \Sigma. \end{aligned} \quad (57)$$

We use approximation (48), introduce $D = f D_f$ and see Eqs. (49), (52) and (55) equivalent to Eqs. (25) – (27). Separating the mean values and fluctuations in operators as in Eqs. (29) we come to Eqs. (30) – (32). Diffusion coefficients for Langevin forces in Eqs. (25) – (27) or (30) – (32) are

$$\begin{aligned} 2D_{nn} = 2\kappa n, \quad 2D_{\Sigma\Sigma} = f[2\kappa D + \gamma_{\perp} N_0 n + (2\kappa + \gamma_{\perp}) N_e] \\ 2D_{DD} = \gamma_{\perp} (N_0 D + 2N_e N_g), \\ 2D_{\Sigma n} = 2D_{n\Sigma} = \kappa \Sigma, \quad 2D_{\Sigma D} = 2D_{D\Sigma} = (\gamma_{\perp}/2) N_0 \Sigma. \end{aligned} \quad (58)$$

Diffusion coefficients followed from GER are all the same as in Eqs. (58), apart from $2D_{DD}$. The term $\gamma_{\perp}2N_eN_g$ is absent in $2D_{DD}$ found in GER.

We make the Fourier transform

$$\delta\hat{\alpha}(t) = \frac{1}{\sqrt{2\pi}} \int_{-\infty}^{\infty} \delta\hat{\alpha}(\omega)e^{-i\omega t}d\omega, \quad \delta\hat{\alpha} = \{\delta\hat{n}, \delta\hat{\Sigma}, \delta\hat{D}\} \quad (59)$$

in the linear equations (30) – (32) and obtain algebraic equations for Fourier-component operators. Solving them we find $\delta\hat{n}(\omega)$, $\delta\hat{\Sigma}(\omega)$. From the relation

$$\langle \delta\hat{n}(\omega)\delta\hat{n}(\omega') \rangle = \delta^2n(\omega)\delta(\omega + \omega') \quad (60)$$

and the similar one for $\delta\hat{\Sigma}(\omega)$, we find the photon number fluctuation spectra $\delta^2n(\omega)$ and $\delta^2\Sigma(\omega)$ with explicit expressions presented in the Appendix. We use the notation ω for the oscillation frequency in Eq. (59) and everywhere below. It should not be confused with the same notation ω in Eqs. (19), (20), and in Eq. (21) for the field spectrum $n(\omega)$, where ω means the deviation from the optical carrier frequency ω_0 .

We obtain the equation for the Fourier component operator $\delta\hat{N}_e(\omega)$ from the linear equation (12). We insert there $\delta\hat{\Sigma}(\omega)$ found above, find $\delta\hat{N}_e(\omega)$ and, from the relation $\langle \delta\hat{N}_e(\omega)\delta\hat{N}_e(\omega') \rangle = \delta^2N_e(\omega)\delta(\omega + \omega')$, obtain the population fluctuation spectrum

$$\delta^2N_e(\omega) = \frac{S_{\Sigma}(\omega)}{(\omega^2 + \gamma_P^2)S(\omega)} + \frac{2D_{N_eN_e}}{\omega^2 + \gamma_P^2}. \quad (61)$$

Eq. (61) is the first-order approximation for $\delta^2N_e(\omega)$ since $S_{\Sigma}(\omega)$ and $S(\omega)$, given in Appendix, are calculated in the zero-order approximation and do not depend on population fluctuations. Writing Eq. (61), we neglect quantum correlations between the population and the polarisation fluctuations of emitters, as we did in [29, 30]. It is a good approximation if the total number of emitters is considerable so that the mean number of photons $n \ll N_{e,g}$.

We take the diffusion coefficient for population fluctuations

$$2D_{N_eN_e} = \gamma_{\parallel}(PN_g + N_e) \quad (62)$$

the same as in [29], the rate equation laser theory [49] and calculations from GER [48].

We find that the photon number variance,

$$\delta^2n = \frac{1}{2\pi} \int_{-\infty}^{\infty} \delta^2n(\omega)d\omega = n(n+1), \quad (63)$$

is the same as for the thermal radiation, consistent with the second-order correlation function $g_2 = 2$ found from the solution of Eqs. (15), (16). The result (63) confirms the correctness of the zero-order diffusion coefficients (58). One can not obtain the result (63) with diffusion coefficients from GER, i.e. without the term $\sim N_eN_g$ in $2D_{DD}$ in Eq. (58).

5 Results and discussion

We calculate zero-order diffusion coefficients (58) and found population fluctuations in the first-order approximation from Eqs. (30) – (32) and (12). Diffusion coefficients (58) let us continue the research of [30] and find the approximate analytical solution of Eqs. (10) – (12) without replacing Eq. (12) with Eq. (24). We will find this solution in the future.

Below we investigate the photon number and the population fluctuations using their spectra and variances. We compare the results for SR LEDs and LEDs without SR.

In examples we take the values of parameters the same as in [29, 30], $\Omega/\gamma_{\parallel} = 34$, $N_0 = 100$, $f = 1/2$, $\kappa/\gamma_{\parallel} = 50$, where $\gamma_{\parallel} = 10^9$ rad/sec and $\kappa = 50 \cdot 10^9$ rad/sec. Similar parameter values can be found, for example, in quantum dot lasers with photonic crystal cavities [50, 51].

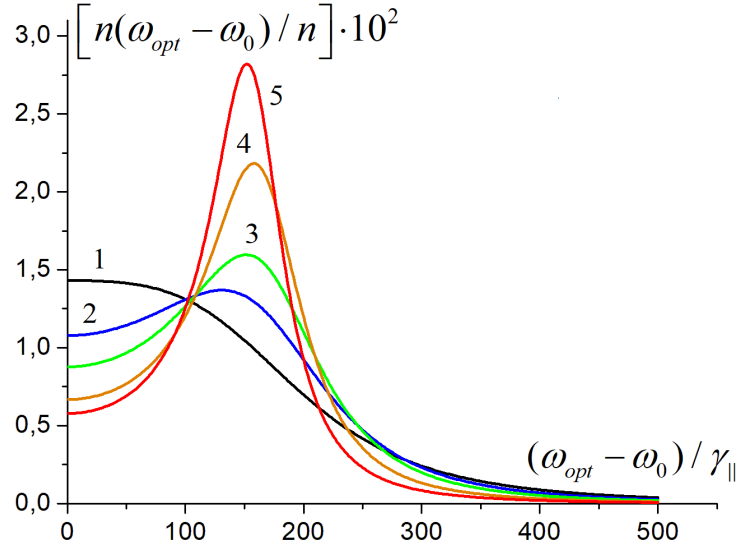


Figure 3: Laser field spectra as functions of the optical frequency $\omega_{opt} = \omega + \omega_0$ for $P = 0.7$, $2\kappa/\gamma_{\perp} = 1/5$ (curve 1), $1/3$ (2), $1/2$ (3), 1 (4) and 2 (5), with other parameters, fixed and given in the text. Parts of spectra with $\omega_{opt} - \omega_0 < 0$ are symmetric with parts with $\omega_{opt} - \omega_0 > 0$ shown in the figure. All curves, but curve 1, have peaks of CRS near $(\omega_{opt} - \omega_0)/\gamma_{\parallel} \approx 150$. CRS peaks grow when the laser approaches the SR regime increasing $2\kappa/\gamma_{\perp}$.

We vary the polarisation relaxation rate γ_{\perp} such that $1/15 < 2\kappa/\gamma_{\perp} < 2$. The case of $2\kappa/\gamma_{\perp} \geq 1$ corresponds to SR lasers, $2\kappa/\gamma_{\perp} \ll 1$ - to lasers without SR [29]. According to Figs. 3 and 4 of [29], the laser at the chosen parameter values has a small mean cavity photon number $n < 1$ and operates in the LED regime for $P \leq 3$. So the weak laser excitation is in the interval $0 < P \leq 3$, and we vary the normalized pump rate P in this interval. The values of all other laser parameters, apart from P and γ_{\perp} , are fixed. Fig. 3 shows the field spectra $n(\omega_{opt} - \omega_0)$ given by Eq. (21). We take $P = 0.7$ and decrease γ_{\perp} from curve 1 to curve 5 in Fig. 3, so $2\kappa/\gamma_{\perp} = 1/5$ (curve 1), $1/3$ (2), $1/2$ (3), 1 (4), 2 (5) and the contribution of SR in the laser grows from the curve 1 to the curve 5. In Fig.3, we see peaks of the collective Rabi splitting (CRS) [33] on curves 2 - 5 with $2\kappa/\gamma_{\perp} \geq 1/3$. The maxima of the CRS peaks grow with $2\kappa/\gamma_{\perp}$, i.e. when the laser approaches the superradiant regime.

Fig. 4 shows the normalized photon number (or, the same, the field intensity) fluctuation spectra $\sqrt{\delta^2 n(\omega)/n(n+1)}$ for the same parameter values as for Fig. 3, $\delta^2 n(\omega)$ is given by Eq. (67) of Appendix. When $2\kappa/\gamma_{\perp}$ is relatively large, as for curves 3, 4 and 5 in Fig.4, we see the sideband CRS peaks on curves. The maxima of the CRS peaks in Fig. 4 correspond approximately to double the values of $\omega_{opt} - \omega_0$ of the CRS peak maxima in the field spectra of Fig. 3. Formally, such a doubling is because $\hat{n} = \hat{a}^+ \hat{a}$ is the binary operator in \hat{a} and \hat{a}^+ . The relative heights of the CRS peaks in the intensity fluctuation spectra in Fig. 4 are smaller than in the field spectra in Fig. 3.

Thus, with the OLM, we found peaks of CRS in the photon number fluctuation spectra of SR LEDs. It supplements the results of [33], where CRS peaks were predicted in the field spectra. CRS peaks in the photon number fluctuation spectra are less visible than in the field spectra (compare Figs. 3 and 4) and must be distinguished from the relaxation oscillation (RO) peaks. CRS and RO peaks are present in the field, and the photon number fluctuation spectra of SR lasers, see [29] and Figs. 3, 4 here. CRS peaks appear at the SR LED regime. RO peaks appear at high excitation when the laser generates coherent radiation. At the high excitation regime, ROs in the field spectra appear as tiny sidebands of the central peak, as in Fig.7a of [29]. The physical reason for the CRS peaks is the collective Rabi splitting. The physical reason for the RO peaks is the energy exchange between the lasing mode and the active medium.

Now we analyze population fluctuations. We see in Eq. (12) two sources of population fluctuations. The first source is fluctuations due to the pump and the energy decay described by the two last terms on the

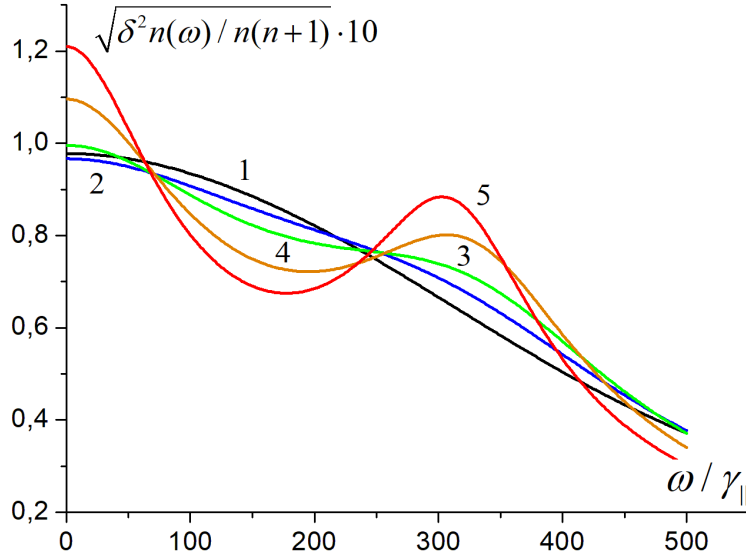


Figure 4: Photon number fluctuation spectra for various γ_{\perp} , the same as in Fig. 3 for curves 1 – 5 correspondingly, and other parameters are given in the text. Curves 3, 4 and 5 have peaks of CRS at frequencies ω approximately two times larger than the values of $\omega_{opt} - \omega_0$ at the maxima of the CRS peaks of the field spectra in Fig. 3.

right in Eq. (12). This source does not depend on the field and the active medium polarization, so it is the same in lasers with and without SR.

The second source is fluctuations of the field-polarization interaction energy $\hat{\Sigma}$, which is described by the term $\sim \delta\hat{\Sigma}$ on the right in Eq. (12). As we see in Eq. (31), $\delta\hat{\Sigma}$ depends on fluctuations $\delta\hat{D}$ of the dipole-dipole interaction energy of emitters. $\delta\hat{D}$ is large in SR lasers, so the contribution of $\delta\hat{\Sigma}$ to the population fluctuations is more significant in SR lasers than in lasers without SR.

Let us see how the contributions of the field-polarization interaction energy and the pump-decay processes to population fluctuations depend on the laser parameters. Fig. 5 shows population fluctuation spectra $\delta^2 \hat{N}_e(\omega)$, given by Eq. (61), for small $2\kappa/\gamma_{\perp} = 1/30 \ll 1$ (the laser without SR, the red curves), and large $2\kappa/\gamma_{\perp} = 2$ (the SR laser, the black curves), for various pump rates $P = 1$ (solid curves) $P = 2$ (dashed curves) and $P = 3$ (dashed-dotted curves).

Fig. 5 shows that the population fluctuation spectra for $P = 1$ and different γ_{\perp} practically coincide. The same is true for $P < 1$. The reason for it is the contribution of the pump-decay fluctuations to population fluctuations, the same for lasers with and without SR, which dominates at small pump $P \leq 1$.

For $P > 1$, population fluctuations in the SR laser with $2\kappa/\gamma_{\perp} = 2$ became larger than in the laser without SR with small $2\kappa/\gamma_{\perp} = 1/30$. The difference in population fluctuations in SR lasers and lasers without SR grows with the pump P ; see in Fig. 5 the difference between the dashed and the dotted-dashed curves of different colours. For $P > 1$, population fluctuations depend more on the field and polarization interaction energy fluctuations. So population fluctuations became larger for the SR laser (the black dashed and dashed-dotted curves) than for the laser without SR (the red dashed and dashed-dotted curves).

With a closer look at Fig. 5, we see that population fluctuations in lasers without SR (red curves) are progressively (and nonlinearly) reduced with the pump. This effect is caused by well-known "population clamping" [43, 52] when the population inversion approaches N_{th} and population fluctuations are reduced with the pump. Reduction of population fluctuations with the pump leads to a well-known reduction of the laser linewidth with a factor of 1/2. See more details, for example, in [29].

Black curves in Fig. (5) show an opposite trend: population fluctuations in SR lasers grow with the pump. We explain this below, together with comments for Fig. 6.

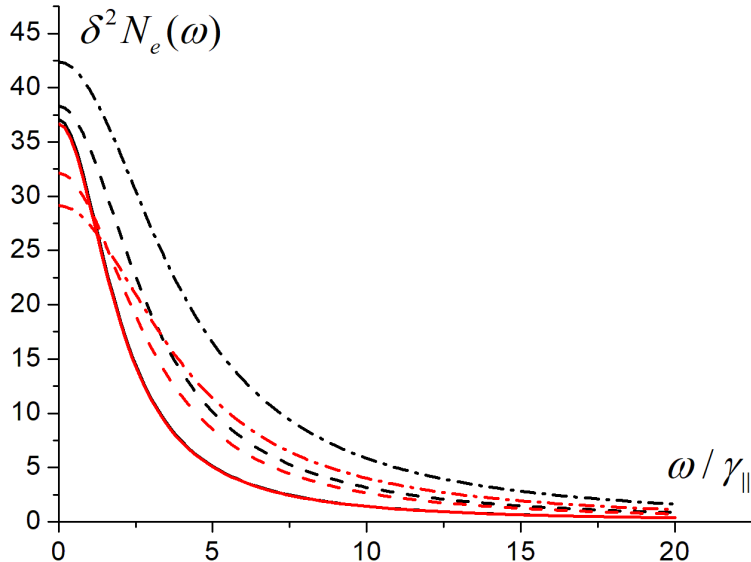


Figure 5: Population fluctuation spectra for the SR laser with $2\kappa/\gamma_{\perp} = 2 > 1$ (black curves) and the laser without SR with $2\kappa/\gamma_{\perp} = 1/30 \ll 1$ (red curves). The normalised pump rate $P = 1$ (solid curves), $P = 2$ (dashed curves) and $P = 3$ (dashed-dotted curves). When $P > 1$ (dashed and dashed-dotted curves), population fluctuations in the SR laser (black curves) are larger than in the laser without SR (red curves). For small $P \leq 1$, population fluctuations depend mostly on the pump and the energy decay, the same for lasers with and without SR, so the population fluctuation spectra for lasers with and without SR for $P \leq 1$ (solid red and black curves) practically coincide.

Fig. 6 shows the population fluctuation dispersion

$$\delta^2 N_e(P) = \frac{1}{2\pi} \int_{-\infty}^{\infty} \delta^2 N_e(\omega) d\omega \quad (64)$$

for $2\kappa/\gamma_{\perp} = 2$ (SR laser, solid curves) and for $2\kappa/\gamma_{\perp} = 1/30$ (laser without SR, dashed curves) and contributions of the pump-decay and the field-polarisation interaction energy fluctuations into $\delta^2 N_e(P)$. The red curves are $\delta^2 N_e(P)$, the blue curves are parts of $\delta^2 N_e$ related to the field and the polarization interaction energy fluctuations, and the black curves are parts of $\delta^2 N_e$ related to the pump-decay fluctuations.

For small pump $P < 1$, the pump-decay fluctuations significantly affect population fluctuations. They do not depend on γ_{\perp} and are the same for lasers with and without SR; the red solid and dashed curves in Fig. 6 coincide. This effect has been used to simplify population fluctuation calculations at small pumps [30]. For $P > 1$, the field-polarization interaction energy's influence on population fluctuations increases, corresponding part of population fluctuations (blue curves in Fig. 6) grew. This part is more significant for SR lasers than those without SR because of the dipole-dipole interaction energy \hat{D} contribution to the field-polarisation interaction energy $\hat{\Sigma}$, see Eqs. (26), (31). \hat{D} and fluctuations $\delta\hat{D}$ are larger for SR lasers than for lasers without SR. So, high dipole-dipole interaction energy fluctuations finally lead to significant population fluctuations in the SR lasers at a large pump.

The contribution of fluctuations of \hat{D} into population fluctuations of SR lasers grows with the pump. It explains the increase of population fluctuations in SR lasers with the pump, as shown by black curves in Fig. 5. Such population fluctuation increase may be suppressed by population clamping at the higher pump. We leave the investigation of this for the future.

Let us discuss the OLM. The exact laser model is, of course, not an ensemble of oscillators. However, OLM is a reasonable approximation for the exact model in cases when population fluctuations can be neglected. OLM correctly predicts some mean values, such as the mean photon number, also for SR lasers [29], and leads to new results, such as the collective Rabi splitting in the field spectra of SR LEDs [33]. Formal justification of the OLM is the coincidence of equations, followed from of OLM, and equations used previously in [29, 30, 33]. We want to provide also physical arguments in favour of OLM, following

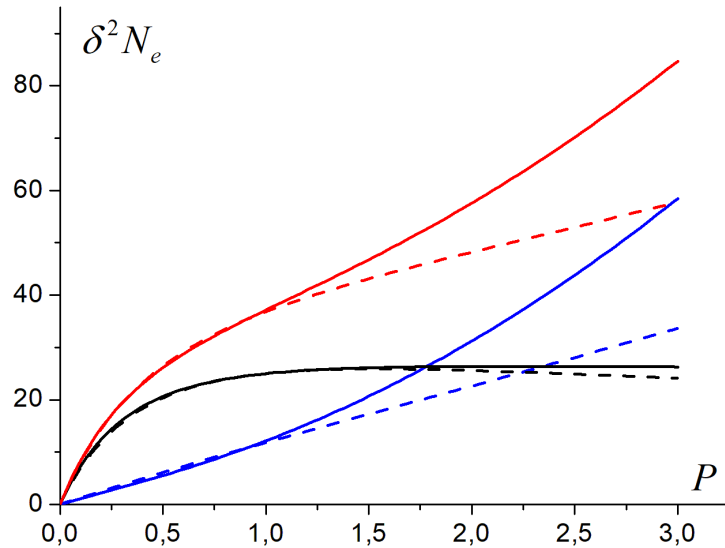


Figure 6: Population fluctuation dispersion is shown for the SR laser (the solid red curve) and the laser without SR (the dashed red curve). Black curves show contributions due to the pump-decay fluctuations, and blue curves are related to the field-polarisation interaction energy fluctuations. Solid curves are for the SR laser; dashed curves are for the laser without SR. The pump-decay fluctuation contribution (black curves) dominates at small pump $P < 1$ and is practically the same for lasers with and without SR. The field-polarisation interaction energy contribution (blue curves) dominates at large pump $P > 2$, which is more prominent for SR lasers than for lasers without SR.

the interpretation of quantum inverted oscillators given in [39]. We quote [39]: “*A fully excited assembly of two-level atoms displays a ladder of equally spaced levels, which extends downwards for many steps. As long as the process is not saturating these levels behave exactly as an inverted oscillator...*”.

The present paper considers two assemblies of N_e excited and N_g emitters in the ground states. There is evidence that the number of emitters in nanolasers is at least an order of magnitude larger than the number of photons at the threshold [10, 50, 53]. So we suppose the mean number n of the cavity photons is small, $n \ll N_{e,g}$ at a low laser excitation. In the OLM, we take a ladder of equally spaced levels, combined from the assembly of N_e excited atoms, and describe it as an inverted oscillator with the operator \hat{b} in the Hamiltonian (38). This oscillator is hardly saturated (downward the energy levels in Fig. 2) by a weak cavity field with the mean number of photons $n \ll N_e$. Similarly, a non-inverted oscillator with the operator \hat{c} combined from the assembly of N_g atoms in the ground states can not be saturated by a weak field with $n \ll N_g$. So with a weak lasing field and neglecting fluctuations of populations of the lasing states, OLM is a physically reasonable approximation for the exact two-level laser model.

Let us consider some single emitter. In the stationary case, transitions between its levels are population fluctuations, which we neglect. So, in our approximation, the emitter makes only virtual transitions. There are precisely N_g emitters in the ground and N_e – in the excited states with no exchange between manifolds of emitters in that states. When an emitter does not come into the excited (or de-excited) state, it does not matter whether it is a two-level system or an oscillator, so we can replace emitters with oscillators in our approximation. Polarization, non-zero at virtual transitions, can be found separately for manifolds of the normal and the inverted oscillators. We do not eliminate polarization adiabatically in a difference with the quantum theory of linear amplifiers [39].

A harmonic oscillator is a primary system in the oscillation theory used in various areas of physics [54]. Many systems can be modelled as interacting harmonic oscillators in mechanics [54, 55], optics [56], chemistry [57] and other physical disciplines. We suggest that OLM will be helpful for the analytical modelling of lasers and other quantum optical systems with an active resonant medium.

6 Conclusion

We present the oscillator laser model – a quantum model of the two-level laser in harmonic oscillators, including *inverted* harmonic oscillators. OLM can be used when population fluctuations of the lasing transitions can be neglected. OLM is a zero-order approximation in the analytical approach of [29, 30, 32, 33]. With OLM, we calculate zero-order diffusion coefficients (58) for approximate equations (30) – (32) for fluctuations in the photon number, the field-polarisation and the dipole-dipole interaction energies of the lasing medium. Diffusion coefficients (58) differ from the well-known ones obtained from generalized Einstein relations for the exact two-level laser model with Hamiltonian (1). Diffusion coefficients (58) provide consistent results, in particular, for the photon number fluctuation variance (63), found from approximate equations (15), (16) and (30) – (32). Zero-order diffusion coefficients are necessary to complete the approximate analytical procedure of solving laser equations [30].

Here with OLM, we calculate the photon number (or the intensity) fluctuation spectra of the lasing field and find the collective Rabi splitting peaks in the intensity fluctuation spectra of the superradiant lasers. This calculation supplements the results of [33], where the collective Rabi splitting peaks have been found in the lasing field spectra.

With the OLM, we calculate the population fluctuations in the first-order approximation, investigate and compare them in the SR lasers and the lasers without SR and suggest the mechanism for the growth of population fluctuations in SR lasers. Population fluctuations at a low laser excitation depend mainly on the pump-decay processes, the same in the lasers with and without SR. When the laser excitation increases, the contribution from the field-polarisation interaction energy to the population fluctuations grows and overcomes the contribution of the pump-decay processes. The dipole-dipole interaction between emitters, large in SR lasers, contribute to the field-polarisation interaction energy. So, when the laser excitation grows, the population fluctuations become larger in SR lasers than in those without SR. Presented results show that population fluctuations play an essential role in SR lasers, as it is for SR [31]. We hope our results will be helpful for experimental studies of population fluctuations in SR lasers, for example, in possible experiments on observing and investigating parameters of the CRS peaks in the lasing field and the field intensity fluctuation spectra.

Appendix

We solve the set of equations (30) – (32) by Fourier-transform and find

$$\delta\hat{n}(\omega) = \frac{-\hat{F}_n [(i\omega - \kappa - \gamma_\perp/2)(i\omega - \gamma_\perp) - 2\Omega^2 fN] + \hat{F}_\Sigma \Omega (i\omega - \gamma_\perp) - \hat{F}_D 2\Omega^2 f}{(i\omega - \kappa - \gamma_\perp/2) [2\kappa\gamma_\perp - \omega^2 - 4\Omega^2 fN - i\omega(2\kappa + \gamma_\perp)]} \quad (65)$$

$$\delta\hat{\Sigma}(\omega) = \frac{\hat{F}_n 2\Omega fN (i\omega - \gamma_\perp) - \hat{F}_\Sigma (i\omega - 2\kappa)(i\omega - \gamma_\perp) + \hat{F}_D (i\omega - 2\kappa) 2\Omega f}{(i\omega - \kappa - \gamma_\perp/2) [2\kappa\gamma_\perp - \omega^2 - 4\Omega^2 fN - i\omega(2\kappa + \gamma_\perp)]}. \quad (66)$$

Using diffusion coefficients (58), we calculate $\langle \delta\hat{n}(\omega)\delta\hat{n}(\omega') \rangle$, $\langle \delta\hat{\Sigma}(\omega)\delta\hat{\Sigma}(\omega') \rangle$, find the photon number fluctuation spectrum $\delta^2 n(\omega)$ in $\langle \delta\hat{n}(\omega)\delta\hat{n}(\omega') \rangle = \delta^2 n(\omega)\delta(\omega + \omega')$,

$$\begin{aligned} \delta^2 n(\omega)S(\omega) &= 2\kappa n \left\{ \left[0.5\gamma_\perp^2 - \omega^2 + \kappa\gamma_\perp(1 - N/N_{th}) \right]^2 + \omega^2(\kappa + 3\gamma_\perp/2)^2 \right\} + \\ &\quad (\kappa\gamma_\perp/2N_{th}) [2\kappa(D + N_e) + \gamma_\perp(N_0 n + N_e)] (\omega^2 + \gamma_\perp^2) + \\ &\quad \kappa^2 \gamma_\perp^3 (N_0 D + 2N_e N_g) / N_{th}^2 + 4\kappa^2 n \left[(\kappa + \gamma_\perp/2) (\omega^2 + \gamma_\perp^2) - \kappa\gamma_\perp^2 N / N_{th} \right] + \\ &\quad 2\kappa^2 \gamma_\perp^3 N_0 / N_{th} \end{aligned} \quad (67)$$

and the spectrum $\delta^2 \Sigma(\omega)$ in $\langle \delta\hat{\Sigma}(\omega)\delta\hat{\Sigma}(\omega') \rangle = \delta^2 \Sigma(\omega)\delta(\omega + \omega')$, it is $\Omega^2 \delta^2 \Sigma(\omega) = S_\Sigma(\omega)/S(\omega)$ with

$$S_\Sigma(\omega) = 2\kappa^3 \gamma_\perp (nN/N_{th}) (\gamma_\perp nN/N_{th} + 4\kappa) (\omega^2 + \gamma_\perp^2) + \quad (68)$$

$$(\kappa\gamma_{\perp}/2N_{th}) [2\kappa D + \gamma_{\perp}N_0n + (2\kappa + \gamma_{\perp})N_e] (\omega^2 + 4\kappa^2) (\omega^2 + \gamma_{\perp}^2) \\ \kappa^2\gamma_{\perp}^3 (\omega^2 + 4\kappa^2) [(N_0D + 2N_eN_g)/N_{th}^2 + 2nN_0/N_{th}]$$

and

$$S(\omega) = [\omega^2 + (\kappa + \gamma_{\perp}/2)^2] \left\{ [2\kappa\gamma_{\perp}(1 - N/N_{th}) - \omega^2]^2 + \omega^2(2\kappa + \gamma_{\perp})^2 \right\}. \quad (69)$$

References

- [1] S. Noda, K. Kitamura, T. Okino, D. Yasuda, Y. Tanaka, *IEEE Journal of Selected Topics in Quantum Electronics* **2017**, *23*, 6 1.
- [2] S. Noda, *Science* **2006**, *314*, 5797 260.
- [3] I. Prieto, J. M. Llorens, L. E. Muñoz-Camúñez, A. G. Taboada, J. Canet-Ferrer, J. M. Ripalda, C. Robles, G. Muñoz-Matutano, J. P. Martínez-Pastor, P. A. Postigo, *Optica* **2015**, *2*, 1 66.
- [4] M. Takiguchi, H. Taniyama, H. Sumikura, M. D. Birowosuto, E. Kuramochi, A. Shinya, T. Sato, K. Takeda, S. Matsuo, M. Notomi, *Opt. Express* **2016**, *24*, 4 3441.
- [5] Y. Ota, M. Kakuda, K. Watanabe, S. Iwamoto, Y. Arakawa, *Opt. Express* **2017**, *25*, 17 19981.
- [6] K. Nozaki, S. Kita, T. Baba, *Opt. Express* **2007**, *15*, 12 7506.
- [7] Y. Yu, W. Xue, E. Semenova, K. Yvind, J. Mork, *Nature Photonics* **2017**, *11*, 2 81.
- [8] Y. Li, L. Wang, L. Li, L. Tong, *Appl. Phys. B* **2019**, *125*, 10 192.
- [9] M. Lermer, N. Gregersen, M. Lorke, E. Schild, P. Gold, J. Mørk, C. Schneider, A. Forchel, S. Reitzenstein, S. Höfling, M. Kamp, *Appl. Phys. Lett.* **2013**, *102*, 5 052114.
- [10] S. Kreinberg, W. W. Chow, J. Wolters, C. Schneider, C. Gies, F. Jahnke, S. Höfling, M. Kamp, S. Reitzenstein, *Light Sci. Appl.* **2017**, *6*, 8 e17030.
- [11] J. Y. Suh, C. H. Kim, W. Zhou, M. D. Huntington, D. T. Co, M. R. Wasielewski, T. W. Odom, *Nano Lett.* **2012**, *12*, 11 5769.
- [12] M. Khajavikhan, A. Simic, M. Katz, J. H. Lee, B. Slutsky, A. Mizrahi, V. Lomakin, Y. Fainman, *Nature* **2012**, *482* 204 EP .
- [13] Y. Kurosaka, S. Iwahashi, Y. Liang, K. Sakai, E. Miyai, W. Kunishi, D. Ohnishi, S. Noda, *Nature Photon.* **2010**, *4*, 7 447.
- [14] W. Zhou, S. Liu, X. Ge, D. Zhao, H. Yang, C. Reuterskiöld-Hedlund, M. Hammar, *IEEE JSTQE* **2019**, *25*, 3 1.
- [15] G. Crosnier, D. Sanchez, S. Bouchoule, P. Monnier, G. Beaudoin, I. Sagnes, R. Raj, F. Raineri, *Nature Photon.* **2017**, *11*, 5 297.
- [16] Y. Sun, S. Combrié, A. De Rossi, F. Bretenaker, *Phys. Rev. A* **2020**, *102* 043503.
- [17] Y. Sun, S. Combrié, F. Bretenaker, A. De Rossi, *Phys. Rev. Lett.* **2019**, *123* 233901.
- [18] Y. I. Khanin, *Fundamentals of laser dynamics*, Cambridge International Science Pub, **2005**.
- [19] A. A. Belyanin, V. V. Kocharovskiy, V. V. Kocharovskiy, *Quant. Semiclass. Opt.: JEOS Part B* **1998**, *10*, 2 L13.
- [20] V. V. Temnov, *Phys. Rev. A* **2005**, *71* 053818.

- [21] M. A. Norcia , J. K. Thompson, *Phys. Rev. X* **2016**, *6* 011025.
- [22] S. A. Schäffer, B. T. R. Christensen, M. R. Henriksen, J. W. Thomsen, *Phys. Rev. A* **2017**, *96* 013847.
- [23] D. Meiser , M. J. Holland, *Phys. Rev. A* **2010**, *81* 033847.
- [24] K. Debnath, Y. Zhang, K. Mølmer, *Phys. Rev. A* **2018**, *98* 063837.
- [25] J. G. Bohnet, Z. Chen, J. M. Weiner, D. Meiser, M. J. Holland, J. K. Thompson, *Nature* **2012**, *484* 78.
- [26] F. Jahnke, C. Gies, M. Afmann, M. Bayer, H. A. M. Leymann, A. Foerster, J. Wiersig, C. Schneider, M. Kamp, S. Höfling, *Nature Commun.* **2016**, *7* 11540.
- [27] D. Bhatti, J. von Zanthier, G. S. Agarwal **2015**, *5* 17335.
- [28] Y. Zhou, F.-l. Li, B. Bai, H. Chen, J. Liu, Z. Xu, H. Zheng, *Phys. Rev. A* **2017**, *95* 053809.
- [29] I. E. Protsenko, A. V. Uskov, E. C. André, J. Mørk, M. Wubs, *New Journal of Physics* **2021**, *23*, 6 063010.
- [30] I. E. Protsenko, A. V. Uskov, *Phys. Rev. A* **2022**, *105* 053713.
- [31] R. J. Glauber, F. Haake, *Phys. Rev. A* **1976**, *13* 357.
- [32] I. Protsenko, P. Domokos, V. Lefèvre-Seguin, J. Hare, J. M. Raimond, L. Davidovich, *Phys. Rev. A* **1999**, *59* 1667.
- [33] E. C. André, I. E. Protsenko, A. V. Uskov, J. Mørk, M. Wubs, *Opt. Lett.* **2019**, *44*, 6 1415.
- [34] C.-P. Hertel, I. V. Schulz, *Atoms, Molecules and Optical Physics 2*, Springer, Berlin, Heidelberg, **2015**.
- [35] M. S. Scully, M. O. Zubairy, *Quantum Optics*, Cambridge University Press, **1997**.
- [36] S. P. Burtsev, I. R. Gabitov, *Phys. Rev. A* **1994**, *49* 2065.
- [37] G. Demeter, *Computer Physics Communications* **2013**, *184*, 4 1203.
- [38] R. J. Glauber, In S. Sarkar, E. R. Pike, editors, *Frontiers in quantum optics*. Hilger, Boston, MA, **1986**.
- [39] S. Stenholm, *Physica Scripta* **1986**, *T12* 56.
- [40] J.-M. Courty, S. Reynaud, *Phys. Rev. A* **1992**, *46* 2766.
- [41] M. J. Collett, C. W. Gardiner, *Phys. Rev. A* **1984**, *30* 1386.
- [42] K. Eberl, M. K. Zundel, *Quantum-dot lasers*, McGraw-Hill Education, **2000**.
- [43] L. Davidovich, *Rev. Mod. Phys.* **1996**, *68* 127.
- [44] M. Sargent, M. O. Scully, W. E. Lamb, *Laser Physics*, London : Addison-Wesley, **1974**.
- [45] C. Gies, J. Wiersig, M. Lorke, F. Jahnke, *Phys. Rev. A* **2007**, *75* 013803.
- [46] M. Travagnin, L. A. Lugiato, *Phys. Rev. A* **2000**, *62* 043813.
- [47] I. E. Protsenko, L. A. Lugiato, *Journ. Semiclass. and Quant. Optics* **1996**, *8* 1067.
- [48] P. L. Kelley, B. Lax, P. E. Tannenwald, *Physics of Quantum Electronics*, McGraw-Hill, Inc., **1966**.

- [49] L. A. Coldren, S. W. Corzine, M. L. Masanovic, *Diode lasers and photonic integrated circuits*, Wiley, 2nd ed., **2012**.
- [50] J. Mørk , G. L. Lippi, *Appl. Phys. Lett.* **2018**, *112*, 14 141103.
- [51] U. Bockelmann , T. Egeler, *Phys. Rev. B* **1992**, *46* 15574.
- [52] M. I. Kolobov, L. Davidovich, E. Giacobino, C. Fabre, *Phys. Rev. A* **1993**, *47* 1431.
- [53] M. A. Carroll, G. D'Alessandro, G. L. Lippi, G.-L. Oppo, F. Papoff, *Phys. Rev. Lett.* **2021**, *126* 063902.
- [54] A. A. Andronov, A. A. Vitt, S. E. Khaikin, *Theory of Oscillators*, Adiwes International Series in Physics. Pergamon, **1966**.
- [55] L. D. Landau, E. M. Lifshitz, *Mechanics, Third Edition: Volume 1 (Course of Theoretical Physics)*, Butterworth-Heinemann, 3 edition, **1976**.
- [56] N. V. Tkachenko, In N. V. Tkachenko, editor, *Optical Spectroscopy*, 15–38. Elsevier Science, Amsterdam, ISBN 978-0-444-52126-2, **2006**, URL <https://www.sciencedirect.com/science/article/pii/B9780444521262500265>.
- [57] R. P. Ozerov, A. A. Vorobyev, In R. P. Ozerov, A. A. Vorobyev, editors, *Physics for Chemists*, 105–167. Elsevier, Amsterdam, ISBN 978-0-444-52830-8, **2007**, URL <https://www.sciencedirect.com/science/article/pii/B9780444528308500040>.